Journal of Electromagnetic Waves and Applications, Volume 10, 1623-1644, 1996

Accurate analysis of scattering from multiple waveguide discontinuities using the coupled-integral equations technique

S. Amari, J. Bornemann, and R. Vahldieck

Laboratory for Lightwave Electronics, Microwaves and Communications (LLiMiC)
Department of Electrical and Computer Engineering
University of Victoria
Victoria B. C. Canada V8W 3P6

Abstract–A Coupled-Integral-Equations Technique (CIET) for the analysis of multiple discontinuities and bifurcations in rectangular waveguides is presented. A set of coupled integral equations for the tangential electric field over the planes of the discontinuities are derived and then solved by the moment method. Basis functions, which include the edge conditions and mirror images in the walls of the waveguide, are used to accelerate convergence of the numerical solution. One or two basis functions are sufficient to accurately determine the reflection and transmission properties of H-plane discontinuities and bifurcations. Reflection and transmission properties of N discontinuities are computed accurately from a single matrix of the order of $3N \times 3N$ instead of cascading the individual generalized scattering matrices whose dimensions increase rapidly as the distances between the discontinuities decrease.

I. INTRODUCTION

Discontinuities in waveguides have been heavily investigated both numerically and analytically over the past five decades. They have also been used, and continue to be used, in a variety of microwave devices such as couplers, filters and matching sections.

Early methods of analysis were essentially analytical in character, geared towards deriving equivalent lumped circuit elements for a given discontinuity. Variational expressions for these lumped elements were established and then used to obtain accurate results with reasonable trial solutions [1,2].

The Mode-Matching Technique (MMT), coupled with the generalized scattering matrix method, was also used by many researchers [3,4]. The moment method was also used by Auda and Harrington [5], by Leog *et.al.* [6] and by Lyapin *et.al.* [7] to investigate scattering from a waveguide discontinuity. Recent work on improving the MMT has focused on including the edge conditions and dealing with the phenomenon of relative convergence [8]. Along these lines, Sorrentino *et.al.* [9] presented and extensive discussion of the numerical properties of inductive and capacitive irises within a modified mode-matching technique which includes the edge conditions. The tangential electric field at the aperture of the iris are expanded in series of weighted Gegenbauer polynomials. A similar approach was used by Rozzi and Mongiardo in the analysis of flange-mounted rectangular waveguide radiators [10]. Omar and Yang also used basis functions which include

the edge conditions in their analysis of multiple windows in a resonant iris for microwave filters applications [11].

In the work reported in the literature up to date, attention is focused on a single discontinuity at a time. The analysis of multiple and successive discontinuities is performed in a modular fashion by cascading the individual generalized scattering matrices or admittance matrices. Although this approach enjoys a high degree of flexibility, as a variety of discontinuities can be analyzed separately and then stitched together, it gives and undue role to the normal modes of the waveguides. The situation becomes even more crucial when the distance between adjacent discontinuities decreases, leading to large individual scattering matrices.

In most applications where multiple discontinuities are used, measured quantities refer to response functions, such as transmission and reflection coefficients, at the "external" ports of the structure. Indeed, two physically different circuits are equivalent if their response functions are equal regardless of their internal structures. The behavior of the electromagnetic field at all internal discontinuities, although important in determining the overall response functions, is of limited interest. The Coupled-Integral-Equations Technique (CIET) used in this paper allows the direct computation of the response functions at the external ports and still accurately describes the electromagnetic field in the entire structure.

In this paper, we reexamine the role played by the individual modes of the waveguide and show how multiple successive discontinuities can be investigated in a single run. The approach relies on the fact that the dominant physics of the problem takes place *at* the discontinuities; the normal modes only provide a means of describing the energy flow. From the uniqueness theorem, specifying the tangential electric field over a closed surface is sufficient to determine the electromagnetic field in the volume enclosed by that surface [12]. The expansion coefficients over the normal modes of a section of a waveguide contained between two consecutive discontinuities, can therefore be expressed in terms of the tangential electric fields at the same discontinuities. The problem is reformulated in terms of these tangential fields instead of the normal modes of the waveguiding sections. By doing so, important information about the edge conditions and mirror images can be straightforwardly incorporated in the theory from the outset. Also, all the normal modes are included in the theory as they are involved only in computing inner products, regardless of the strength of the interactions between the discontinuities.

In order not bury the main idea of the technique in algebraic manipulations, in this paper, we only consider H-plane discontinuities. We investigate the reflection properties of an infinitely long asymmetric bifurcation, a bifurcation of finite length, and finally cascades of two and three septums of finite length. In all cases, the efficiency and accuracy of the technique is documented.

II. SCATTERING OF TE_{10} FROM TWO SEPTUMS

The structure under consideration is shown in Figure 1a. It consists of a rectangular waveguide of cross section a × b and two H-plane septums of thickness d_1 and d_3 and height $a - a_1$. The two septums are separated by a distance d_2. We assume that all metals are perfectly conducting and that only the fundamental mode TE_{10} is incident from left side.

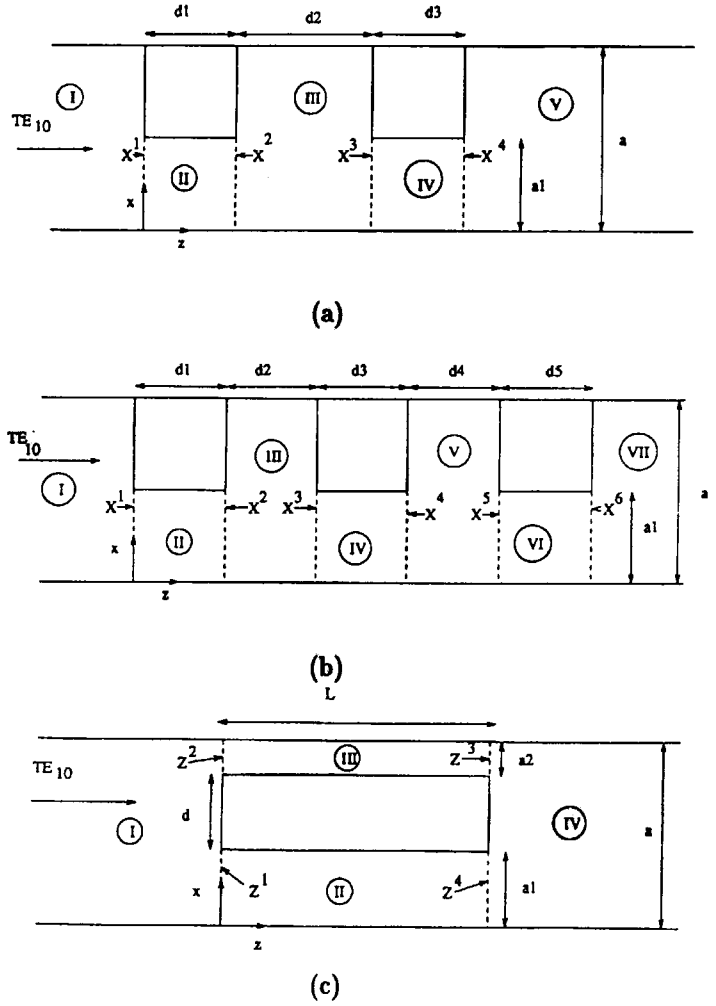

Figure 1: Subdivision of structure and coordinate systems. a) two septums, b) three septums and c) finite length bifurcation.

In the standard Mode Matching Technique (MTT), the structure is analyzed by determining matrix representations for the individual discontinuities, I-II, II-III, III-IV and IV-V respectively, and then cascading the individual matrix representations. The efficiency of the method can be improved by including the edge conditions in the analysis of each discontinuity and the fact that only a

finite number of "accessible" modes are important in the interaction between two neighboring discontinuities [13]. It is, however, not obvious how a proper number of "accessible" modes is to be rigorously determined beforehand.

In the present method, we take another approach to the problem. To guarantee numerical efficiency, the method must include the edge conditions as well as any other pivotal information about the electromagnetic field. In addition, it must accurately take into account the interaction between neighboring discontinuities regardless of their separation. Fortunately, both requirements can be incorporated in the present method.

Let us assume that the tangential electric field at the gaps of the interfaces are denoted by $X^{(1)}(x)$, $X^{(2)}(x)$, $X^{(3)}(x)$, $X^{(4)}(x)$ respectively (see Figure 1a). When only the TE_{10} mode is incident (with amplitude equal to unity) on this structure, only TE_{m0} modes are excited [4]. The electromagnetic field in each of the regions I to IV can be expanded in a series of forward and backward traveling normal modes whereas that in region V has only forward traveling modes. Therefore, the transverse components of the electric and magnetic fields in each of the five regions can be written as

$$E_y^I(x,z) = \sin[\pi\frac{x}{a}]e^{-jk_1^I z} + \sum_{m=1}^{\infty} B_m^I \sin[m\pi\frac{x}{a}]e^{jk_m^I z} \tag{1.a}$$

$$H_x^I(x,z) = -Y_1^I \sin[\pi\frac{x}{a}]e^{-jk_1^I z} + \sum_{m=1}^{\infty} Y_m^I B_m^I \sin[m\pi\frac{x}{a}]e^{jk_m^I z} \tag{1.b}$$

$$E_y^{II}(x,z) = \sum_{m=1}^{\infty} [B_m^{II} e^{jk_m^I z} + F_m^{II} e^{-jk_m^{II} z}] \sin[m\pi\frac{x}{a_1}] \tag{2.a}$$

$$H_x^{II}(x,z) = \sum_{m=1}^{\infty} Y_m^{II} [B_m^{II} e^{jk_m^{II} z} - F_m^{II} e^{-jk_m^{II} z}] \sin[m\pi\frac{x}{a_1}] \tag{2.b}$$

$$E_y^{III}(x,z) = \sum_{m=1}^{\infty} [B_m^{III} e^{jk_m^{III} z} + F_m^{III} e^{-jk_m^{III} z}] \sin[m\pi\frac{x}{a}] \tag{3.a}$$

$$H_x^{III}(x,z) = \sum_{m=1}^{\infty} Y_m^{III} [B_m^{III} e^{jk_m^{III} z} - F_m^{III} e^{-jk_m^{III} z}] \sin[m\pi\frac{x}{a}] \tag{3.b}$$

$$E_y^{IV}(x,z) = \sum_{m=1}^{\infty} [B_m^{IV} e^{jk_m^{IV} z} + F_m^{IV} e^{-jk_m^{IV} z}] \sin[m\pi\frac{x}{a_1}] \tag{4.a}$$

$$H_x^{IV}(x,z) = \sum_{m=1}^{\infty} Y_m^{IV} [B_m^{IV} e^{jk_m^{IV} z} - F_m^{IV} e^{-jk_m^{IV} z}] \sin[m\pi\frac{x}{a_1}] \tag{4.b}$$

and

$$E_y^V(x,z) = \sum_{m=1}^{\infty} F_m^V e^{-jk_m^V z} \sin[m\pi\frac{x}{a}] \tag{5.a}$$

$$H_x^V(x,y) = -\sum_{m=1}^{\infty} Y_m^V F_m^V e^{-jk_m^V z} \sin[m\pi \frac{x}{a}] \tag{5.b}$$

Here

$$k_m^I = k_m^{III} = k_m^V = \begin{cases} +\sqrt{\omega^2\epsilon_0\mu_0 - (\frac{m\pi}{a})^2}, & \text{propagating mode} \\ -j\sqrt{(\frac{m\pi}{a})^2 - \omega^2\epsilon_0\mu_0}, & \text{evanescent mode} \end{cases} \tag{6.a}$$

$$k_m^{II} = k_m^{IV} = \begin{cases} +\sqrt{\omega^2\epsilon_0\mu_0 - (\frac{m\pi}{a-a_1})^2}, & \text{propagating mode} \\ -j\sqrt{(\frac{m\pi}{a-a_1})^2 - \omega^2\epsilon_0\mu_0}, & \text{evanescent mode} \end{cases} \tag{6.b}$$

$$Y_m^I = Y_m^{III} = Y_m^V = \frac{k_m^I}{\omega\mu_0} \tag{7.a}$$

and

$$Y_m^{II} = Y_m^{IV} = \frac{k_m^{II}}{\omega\mu_0} \tag{7.b}$$

The boundary conditions of the problem consist in the vanishing of the tangential (transverse) electric field over the metallic surfaces at each discontinuity and the continuity of the tangential electric and magnetic fields over the gaps. By choosing the functions $X^i(x)$ to vanish on the metallic surfaces of the discontinuities, the first boundary condition of the tangential electric field is automatically satisfied, i.e., $X_i(x)$ must satisfy

$$X^{(i)}(x) = 0, \quad i = 1,2,3,4, \quad a_1 \le x \le a \tag{8}$$

Since the quantities $X^{(i)}(x)$ are equal to the tangential electric field at the discontinuities, they can be used to eliminate the modal expansion coefficients, B_m^i and F_m^i. More precisely, by equating the expressions given in equations (1) to (5) to the appropriate functions $X^{(i)}(x)$ we get

$$B_m^I = -\delta_{m1} + \tilde{X}_1^{(1)}(m) \tag{9}$$

$$\begin{aligned} B_m^{II} &= j\frac{e^{-jk_m^{II}d_1}\tilde{X}_2^{(1)}(m) - \tilde{X}_2^{(2)}(m)}{2\sin[k_m^{II}d_1]} \\ F_m^{II} &= j\frac{\tilde{X}_2^{(2)}(m) - e^{jk_m^{II}d_1}\tilde{X}_2^{(1)}(m)}{2\sin[k_m^{II}d_1]} \end{aligned} \tag{10}$$

$$\begin{aligned} B_m^{III} &= je^{-jk_m^I d_1}\frac{e^{-jk_m^I d_2}\tilde{X}_1^{(2)}(m) - \tilde{X}_1^{(3)}(m)}{2\sin[k_m^I d_2]} \\ F_m^{III} &= je^{jk_m^I d_1}\frac{\tilde{X}_1^{(3)}(m) - e^{jk_m^I d_2}\tilde{X}_1^{(2)}(m)}{2\sin[k_m^I d_2]} \end{aligned} \tag{11}$$

$$\begin{aligned} B_m^{IV} &= je^{-jk_m^{II}(d_1+d_2)}\frac{e^{-jk_m^{II}d_3}\tilde{X}_2^{(3)}(m) - \tilde{X}_2^{(4)}(m)}{2\sin[k_m^{II}d_3]} \\ F_m^{IV} &= je^{jk_m^{II}(d_1+d_2)}\frac{\tilde{X}_2^{(4)}(m) - e^{jk_m^{II}d_2}\tilde{X}_2^{(3)}(m)}{2\sin[k_m^{II}d_3]} \end{aligned} \tag{12}$$

and

$$F_m^{IV} = e^{jk_m^V(d_1+d_2+d_3)}\tilde{X}_1^{(4)}(m). \tag{13}$$

The following notations were introduced for convenience

$$\begin{aligned}\tilde{X}_1^{(i)}(m) &= \frac{2}{a}\int_0^{a_1} X^{(i)}(x)\sin[m\pi\frac{x}{a}]dx \\ \tilde{X}_2^{(i)}(m) &= \frac{2}{a_1}\int_0^{a_1} X^{(i)}(x)\sin[m\pi\frac{x}{a_1}]dx\end{aligned} \tag{14}$$

The unknown functions $X^{(i)}(x)$ will be determined from the requirement that the tangential magnetic field be continuous at each of the four interfaces. By using the expressions of the modal expansion coefficients as given by equations (9)-(13), in the modal expansions of the tangential magnetic field, we obtain a set of coupled integral equations in the functions $X^{(i)}(x)$. More precisely, from the continuity of H_x at interface I-II we get

$$\begin{aligned}-j\sum_{m=1}^{\infty} Y_m^{II}[\tilde{X}_2^{(1)}(m)\cot(k_m^{II}d_1) - \frac{\tilde{X}_2^{(2)}(m)}{\sin[k_m^{II}d_1]}]\sin[m\pi\frac{x}{a_1}] \\ + \sum_{m=1}^{\infty} Y_m^I\tilde{X}_1^{(1)}(m)\sin[m\pi\frac{x}{a}] = 2Y_1^I\sin(\pi\frac{x}{a}], \quad 0\le x\le a_1.\end{aligned} \tag{15}$$

Similarly, from the continuity of H_x at interface II-III

$$\begin{aligned}\sum_{m=1}^{\infty} Y_m^{II}[\frac{\tilde{X}_2^{(1)}(m)}{\sin[k_m^{II}d_1]} - \tilde{X}_2^{(2)}(m)\cot(k_m^{(2)}d_1)]\sin[m\pi\frac{x}{a_1}] \\ - \sum_{m=1}^{\infty} Y_m^I[\tilde{X}_1^{(2)}(m)\cot(k_m^I d_2) - \frac{\tilde{X}_1^{(3)}(m)}{\sin[k_m^I d_2]}]\sin[m\pi\frac{x}{a}] = 0, \quad 0\le x\le a_1.\end{aligned} \tag{16}$$

From the continuity of H_x at interface III-IV,

$$\begin{aligned}\sum_{m=1}^{\infty} Y_m^I[\frac{\tilde{X}_1^{(2)}(m)}{\sin[k_m^I d_2]} - \tilde{X}_1^{(3)}(m)\cot(k_m^I d_2)]\sin[m\pi\frac{x}{a}] \\ - \sum_{m=1}^{\infty} Y_m^{II}[\tilde{X}_2^{(3)}(m)\cot(k_m^{II}d_3) - \frac{\tilde{X}_2^{(4)}(m)}{\sin[k_m^{II}d_3]}]\sin[m\pi\frac{x}{a_1}] = 0, \quad 0\le x\le a_1.\end{aligned} \tag{17}$$

And finally from interface IV-V

$$\begin{aligned}j\sum_{m=1}^{\infty} Y_m^{II}[\frac{\tilde{X}_2^{(3)}(m)}{\sin[k_m^{II}d_3]} - \tilde{X}_2^{(4)}(m)\cot(k_m^{II}d_3)]\sin[m\pi\frac{x}{a_1}] \\ + \sum_{m=1}^{\infty} Y_m^I[\tilde{X}_1^{(4)}(m)\sin[m\pi\frac{x}{a}] = 0, \qquad 0\le x\le a_1.\end{aligned} \tag{18}$$

Equations (15) to (18) are a set of linear coupled integral equations from which the scattering properties of the structure are determined. For example, the reflection

coefficient is given by B_1^I, equation (9), whereas equation (13) gives the transmission coefficient. The intermediate regions are accurately taken into account although we are only interested in the overall performance of the structure.

It can now be easily seen how the edge conditions can be included in the formulation from the outset and at each one of the discontinuities simultaneously. It is also evident that all the modes of the individual sections of the waveguides are included as they appear only in computing the sums (inner products in the moment method solution) which are tested for convergence.

III. METHOD OF SOLUTION

The four coupled integral equations (15)-(18) can be solved following the standard moment method for a single integral equation [14]. Each of the unknown functions is expanded in a series of basis functions and then some form of projection is performed on each of the integral equations. Since the gaps of the septums are all assumed equal, we use the same basis functions to expand the fields at the interfaces. Let $B_i(x)$ denote a generic element of this set of basis functions. The unknown functions $X^{(i)}(x)$ are written in the forms

$$X^{(i)}(x) = \sum_{k=1}^{M} c_k^{(i)} B_k(x), \quad i = 1,2,3,4. \tag{19}$$

Using equations (19) in equations (15) to (18) and applying Galerkin's method we get four sets of linear equations in the expansion coefficients $c_k^{(i)}$

$$[A][c^{(1)}] + [B][c^{(2)}] = [U] \tag{20.a}$$

$$[C][c^{(1)}] + [D][c^{(2)}] + [E][c^{(3)}] = 0 \tag{20.b}$$

$$[F][c^{(2)}] + [G][c^{(3)}] + [H][c^{(4)}] = 0 \tag{20.c}$$

$$[I][c^{(3)}] + [J][c^{(4)}] = 0 \tag{20.d}$$

The entries of the matrices in equations (20) are given by

$$[A]_{kl} = \sum_{m=1}^{\infty} [Y_m^I \tilde{B}_{k1}(m)\tilde{B}_{l1}(m) - j\frac{a_1}{a} Y_m^{II} \tilde{B}_{k2}(m)\tilde{B}_{l2}(m)\cot(k_m^{II} d_1)] \tag{21.a}$$

$$[B]_{kl} = j\frac{a_1}{a} \sum_{m=1}^{\infty} Y_m^{II} \frac{\tilde{B}_{k1}(m)\tilde{B}_{l1}(m)}{\sin[k_m^{II} d_1]} \tag{21.b}$$

$$[U]_k = 2Y_1^I \tilde{B}_{k1}(1) \tag{21.c}$$

$$[C]_{kl} = -j[B]_{kl} \tag{22.a}$$

$$\begin{aligned}[D]_{kl} = -\sum_{m=1}^{\infty} &[Y_m^I \cot(k_m^I d_2)\tilde{B}_{k1}(m)\tilde{B}_{l1}(m) \\ &+ \frac{a_1}{a} Y_m^{II} \cot(k_m^{II} d_1)\tilde{B}_{k1}(m)\tilde{B}_{l1}(m)]\end{aligned} \tag{22.b}$$

$$[E]_{kl} = \sum_{m=1}^{\infty} Y_m^I \frac{\tilde{B}_{k1}(m)\tilde{B}_{l1}(m)}{\sin[k_m^I d_2]} \tag{22.c}$$

$$[F]_{kl} = [E]_{kl} \tag{23.a}$$

$$\begin{aligned}[G]_{kl} = -\sum_{m=1}^{\infty} [&Y_m^I \cot(k_m^I d_2)\tilde{B}_{k1}(m)\tilde{B}_{l1}(m) \\ &+ \frac{a_1}{a} Y_m^{II} \cot(k_m^{II} d_3)\tilde{B}_{k1}(m)\tilde{B}_{l1}(m)]\end{aligned} \tag{23.b}$$

$$[H]_{kl} = \frac{a_1}{a} \sum_{m=1}^{\infty} Y_m^{II} \frac{\tilde{B}_{k2}(m)\tilde{B}_{l2}(m)}{\sin[k_m^{II} d_3]} \tag{23.c}$$

$$[I]_{kl} = j[H]_{kl} \tag{24.a}$$

and

$$[J]_{kl} = \sum_{m=1}^{\infty} [Y_m^I \tilde{B}_{k1}(m)\tilde{B}_{l1}(m) - j\frac{a_1}{a} Y_m^{II} \tilde{B}_{k2}(m)\tilde{B}_{l2}(m)\cot(k_m^{II} d_3)] \tag{24.b}$$

To complete the solution, and guarantee numerical efficiency, a judicious choice of basis functions must be made. The tangential component of the electric field, E_y, at each of the interfaces has a singularity of the form $x^{2/3}$ at $x = a_1$ and vanishes as x^1 at $x = 0$ [15]. Taking into account the presence of the electric wall at $x = 0$, we use the following set of basis functions

$$B_k(x) = \frac{\sin[k\pi \frac{x}{a_1}]}{[1 - (\frac{x}{a_1})^2]^{1/3}}, \quad k = 1, 2, 3, \ldots \tag{25}$$

The transformed functions $\tilde{B}(m)$ are expressible in terms of Bessel functions of the first kind of order 1/6, namely [16]

$$\tilde{B}_{k1}(m) = \frac{1}{2}\frac{a_1}{a}\Gamma(1/2)\Gamma(2/3)[\frac{J_{1/6}(\pi|m\frac{a_1}{a} - k|)}{(\pi/2|m\frac{a_1}{a} - k|)^{1/6}} - \frac{J_{1/6}(\pi(m\frac{a_1}{a} + k))}{(\pi/2(m\frac{a_1}{a} + k|)^{1/6}}] \tag{26.a}$$

and

$$\tilde{B}_{k2}(m) = \frac{1}{2}\Gamma(1/2)\Gamma(2/3)[\frac{J_{1/6}(\pi|m - k|)}{(\pi/2|m - k|)^{1/6}} - \frac{J_{1/6}(\pi(m + k))}{(\pi/2(m + k|)^{1/6}}]. \tag{26.b}$$

Once the expansion coefficients are determined, the reflected power at interface I-II is easily computed from equation (9). Similarly, the power transmitted from region I to region V is obtained from equation (13).

As the technique shows, the performance of the structure, i.e., its scattering properties are computable directly, in one step, without recourse to the individual matrix representations of each discontinuity. Also, since the modes of the waveguides are summed to compute the matrix elements in equations (21)-(24), and tested for convergence, the strength of the interaction between adjacent discontinuities is also accurately accounted for. The phenomenon of relative convergence is not encountered either as the sums are not truncated at a fixed threshold but rather tested for convergence.

The extension of the formulation to situations where more than one tangential component of the electric field are present, such as double plane discontinuities and circular waveguides, is straightforward although the algebra is admittedly more cumbersome.

The case of three septums can be analyzed following similar steps. Appendix A summarizes the main results of the analysis and gives the expressions of the matrices involved. It becomes evident that large numbers of discontinuities can be effectively handled by the CIET.

In the next section, we show how a bifurcation of finite length can also be accurately investigated using the present technique.

IV. BIFURCATION OF FINITE LENGTH

Bifurcations in waveguides are often encountered in duplexers and power dividers and combiners. In this section, we present an analysis of an H-plane bifurcation of finite length using the Coupled-Integral-Equations Technique (CIET).

The structure under consideration is shown in Figure 1c. The bifurcation of thickness d and length L is illuminated by the fundamental mode TE_{10} from the left side. We are concerned with the reflection and transmission properties of the structure.

Using the standard Mode Matching Technique (MMT), one would determine the generalized scattering matrices of the individual discontinuities and then, from these, compute the scattering properties of the overall structure. Here we determine the reflected and transmitted powers directly.

As in the step discontinuities, we expand the fields in each region in modal series. In region I there are reflected waves in addition to the incident excitation TE_{10} whereas the fields in regions II and III are a superposition of forward and backward traveling waves. In region IV there are only forward traveling waves. The fields in regions I and IV have the same expressions as those given by equations (3) and (4). In regions II and III we have the following expansions

$$E_y^{II}(x,z) = \sum_{m=1}^{\infty} [B_m^{II} e^{jk_m^{II} z} + F_m^{II} e^{-jk_m^{II} z}] \sin[m\pi \frac{x}{a_1}] \tag{27.a}$$

$$H_x^{II}(x,z) = \sum_{m=1}^{\infty} Y_m^{II} [B_m^{II} e^{jk_m^{II} z} - F_m^{II} e^{-jk_m^{II} z}] \sin[m\pi \frac{x}{a_1}] \tag{27.b}$$

$$E_y^{III}(x,z) = \sum_{m=1}^{\infty} [B_m^{III} e^{jk_m^{III} z} + F_m^{III} e^{-jk_m^{III} z}] \sin[m\pi \frac{x-d-a_1}{a_2}] \tag{28.a}$$

and

$$H_x^{III}(x,z) = \sum_{m=1}^{\infty} Y_m^{III} [B_m^{III} e^{jk_m^{III} z} - F_m^{III} e^{-jk_m^{III} z}] \sin[m\pi \frac{x-d-a_1}{a_2}] \tag{28.b}$$

In order to include the edge conditions at each of the discontinuities at z=0 and z=L, we introduce unknown functions which represent the tangential electric fields

at each of the four gaps. Let

$$Z^{(1)}(x) = E_y^{II}(x, z = 0), \quad 0 \le x \le a_1 \tag{29.a}$$

$$Z^{(2)}(x) = E_y^{III}(x, z = 0), \quad a_1 + d \le x \le a \tag{29.b}$$

$$Z^{(3)}(x) = E_y^{II}(x, z = L), \quad 0 \le x \le a_1 \tag{29.c}$$

$$Z^{(4)}(x) = E_y^{III}(x, z = L), \quad a_1 + d \le x \le a \tag{29.d}$$

Using the modal expansions of the tangential electric field in the different regions, we can rewrite their modal expansion coefficients in terms of the unknown functions $Z^{(i)}$. The algebra is straightforward resulting in the following equations

$$B_m^I = -\delta_{m1} + \tilde{Z}_1^{(1)}(m) + \tilde{Z}_1^{(2)}(m) \tag{30}$$

$$B_m^{II} = j\frac{\tilde{Z}_2^{(1)}(m)e^{-jk_m^{II}L} - \tilde{Z}_2^{(3)}}{2\sin[k_m^{II}L]} \tag{31.a}$$

$$F_m^{II} = j\frac{\tilde{Z}_2^{(3)}(m) - e^{jk_m^{II}L}]\tilde{Z}_2^{(1)}(m)}{2\sin[k_m^{II}L]} \tag{31.b}$$

$$B_m^{III} = j\frac{\tilde{Z}_3^{(2)}(m)e^{-jk_m^{III}L} - \tilde{Z}_3^{(4)}}{2\sin[k_m^{III}L]} \tag{31.c}$$

$$F_m^{III} = j\frac{\tilde{Z}_3^{(4)}(m) - e^{jk_m^{III}L}]\tilde{Z}_3^{(2)}(m)}{2\sin[k_m^{III}L]} \tag{31.d}$$

and

$$F_m^{IV} = e^{jk_m^I L}[\tilde{Z}_1^{(3)}(m) + \tilde{Z}_1^{(4)}(m)] \tag{31.e}$$

Here the following notations were introduced

$$\tilde{Z}_1^{(1,3)}(m) = \frac{2}{a}\int_0^{a_1} Z^{(1,3)}(x)\sin[m\pi\frac{x}{a}]dx \tag{32.a}$$

$$\tilde{Z}_1^{(2,4)}(m) = \frac{2}{a}\int_{a_1+d}^{a} Z^{(2,4)}(x)\sin[m\pi\frac{x}{a}]dx \tag{32.b}$$

$$\tilde{Z}_2^{(1,3)}(m) = \frac{2}{a_1}\int_0^{a_1} Z^{(1,3)}(x)\sin[m\pi\frac{x}{a_1}]dx \tag{32.c}$$

$$\tilde{Z}_3^{(2,4)}(m) = \frac{2}{a_2}\int_{a_1+d}^{a} Z^{(2,4)}(x)\sin[m\pi\frac{x - a_1 - d}{a_2}]dx \tag{32.d}$$

To establish a set of coupled intergal equations for the unknown quantities $Z^{(i)}(x)$, equations (30) and (31) are used in the modal expansions of the tangential magnetic fields, and then the continuity of H_x is enforced at each discontinuity. More specifically, from the continuity of H_x at interface I-II,

$$\sum_{m=1}^{\infty} jY_m^{II}[\frac{\tilde{Z}_2^{(3)}(m)}{\sin[k_m^{II}L]} - \cot(k_m^{II}L)\tilde{Z}_2^{(3)}(m)]\sin[m\pi\frac{x}{a_1}]$$

$$+ \sum_{m=1}^{\infty} Y_m^I[\tilde{Z}_1^{(1)}(m) + \tilde{Z}_1^{(2)}(m)]\sin[m\pi\frac{x}{a}] = 2Y_1^I\sin[\pi\frac{x}{a}], \quad 0 \le x \le a_1 \tag{33}$$

The continuity of H_x at interface I-III leads to

$$\sum_{m=1}^{\infty} jY_m^{III}[\frac{\tilde{Z}_3^{(2)}(m)}{\sin[k_m^{III}L]} - \cot(k_m^{III}L)\tilde{Z}_3^{(4)}(m)]\sin[m\pi\frac{x-a_1-d}{a_2}] + \sum_{m=1}^{\infty} Y_m^I[\tilde{Z}_1^{(1)}(m) + \tilde{Z}_1^{(2)}(m)]\sin[m\pi\frac{x}{a}] = 2Y_1^I\sin[\pi\frac{x}{a}], \quad a_1 + d \le x \le a \tag{34}$$

Similarly, the continuity of H_x at interface II-IV gives

$$\sum_{m=1}^{\infty} jY_m^{II}[\frac{\tilde{Z}_2^{(1)}(m)}{\sin[k_m^{II}L]} - \cot(k_m^{II}L)\tilde{Z}_2^{(3)}(m)]\sin[m\pi\frac{x}{a_1}] + \sum_{m=1}^{\infty} Y_m^I[\tilde{Z}_1^{(3)}(m) + \tilde{Z}_1^{(4)}(m)]\sin[m\pi\frac{x}{a}] = 0, \quad 0 \le x \le a_1 \tag{35}$$

And finally, the continuity of H_x at interface III-IV leads to

$$\sum_{m=1}^{\infty} jY_m^{III}[\frac{\tilde{Z}_3^{(4)}(m)}{\sin[k_m^{III}L]} - \cot(k_m^{III}L)\tilde{Z}_3^{(2)}(m)]\sin[m\pi\frac{x-a_1-d}{a_2}] + \sum_{m=1}^{\infty} Y_m^I[\tilde{Z}_1^{(3)}(m) + \tilde{Z}_1^{(4)}(m)]\sin[m\pi\frac{x}{a}] = 0, \quad a_1 + d \le x \le a \tag{36}$$

These coupled integral equations are solved by the moment method as in the case of the the step discontinuities. Let $P_k(x)$ and $Q_k(x)$ be basis functions for the tangential electric field at the gaps of regions II and III respectively. If the functions $Z^{(i)}(x)$ are expanded in series of the form

$$Z^{(1)}(x) = \sum_{k=1}^{M} a_k^{(1)}P_k(x) \tag{37.a}$$

$$Z^{(2)}(x) = \sum_{k=1}^{M} a_k^{(2)}Q_k(x) \tag{37.b}$$

$$Z^{(3)}(x) = \sum_{k=1}^{M} a_k^{(3)}P_k(x) \tag{37.c}$$

$$Z^{(4)}(x) = \sum_{k=1}^{M} a_k^{(4)}Q_k(x), \tag{37.d}$$

and Galerkin's method applied to each of the integral equations (33) to (36), we get four sets of linear equations in the expansion coefficients $a_k^{(i)}$.

$$[A][a^{(1)}] + [B][a^{(2)}] + [C][a^{(3)}] = [U] \tag{38.a}$$

$$[D][a^{(1)}] + [E][a^{(2)}] + [F][a^{(4)}] = [V] \tag{38.b}$$

$$[G][a^{(1)}] + [H][a^{(3)}] + [K][a^{(4)}]] = [0] \tag{38.c}$$

$$[L][a^{(2)}] + [M][a^{(3)}] + [N][a^{(4)}] = [0] \tag{38.d}$$

The entries of the matrices in equations (38) are given by

$$[A]_{kl} = \sum_{m=1}^{\infty} [Y_m^I \tilde{P}_{k1}(m)\tilde{P}_{l1}(m) - j\frac{a_1}{a} Y_m^{II} P_{k2}(m)\tilde{P}_{l2}(m)\cot(k_m^{II}L)] \tag{39.a}$$

$$[B]_{kl} = \sum_{m=1}^{\infty} \tilde{P}_{k1}(m)\tilde{Q}_{l1}(m) \tag{39.b}$$

$$[C]_{kl} = j\frac{a_1}{a} \sum_{m=1}^{\infty} Y_m^{II} \frac{\tilde{P}_{k2}(m)\tilde{P}_{l2}(m)}{\sin[k_m^{II}L]} \tag{39.c}$$

$$[U]_k = 2Y_1^I \tilde{P}_{k1}(1) \tag{39.d}$$

$$[D]_{kl} = [B]_{lk} \tag{40.a}$$

$$[E]_{kl} = \sum_{m=1} [Y_m^I \tilde{Q}_{k1}(m)\tilde{Q}_{l1}(m) - j\frac{a_2}{a} Y_m^{III} \tilde{Q}_{k3}(m)\tilde{Q}_{l3}(m)\cot(k_m^{III}L)] \tag{40.b}$$

$$[F]_{kl} = j\frac{a_2}{a} \sum_{m=1}^{\infty} Y_m^{III} \frac{\tilde{Q}_{k3}(m)\tilde{Q}_{l3}(m)}{\sin[k_m^{III}L]} \tag{40.c}$$

$$[V]_k = 2Y_1^I \tilde{Q}_{k1}(1) \tag{40.d}$$

$$[G] = [C] \tag{41.a}$$

$$[H] = [A] \tag{41.b}$$

$$[K] = [B] \tag{41.c}$$

$$[L] = [F] \tag{42.a}$$

$$[M] = [D] \tag{42.b}$$

$$[N] = [E] \tag{42.c}$$

From the expressions of these matrices, it is clear that one needs to compute only the matrices [A], [B], [C], [E] and [F], which are all symmetric except for [B]. It will be seen that only one or two basis functions are necessary to obtain accurate results for the reflected and transmitted powers. This reduces the number of sums to only 16 regardless of the strength of the interactions between the discontinuities when only the fundamental mode TE_{10} is propagating. There is a considerable reduction in the numerical burden and an increase in the numerical efficiency over the standard Mode-Matching Technique (MMT).

The choice of basis functions for the bifurcation is similar to the step discontinuity. A set of basis functions which take into account the edge conditions as well as the mirror images in the electric walls of the waveguides is given by

$$P_k(x) = \frac{\sin[k\pi\frac{x}{a_1}]}{(1-(\frac{x}{a_1})^2]^{1/3}}, \quad k = 1, 2, 3, \ldots \tag{43}$$

and

$$Q_k(x) = \frac{\sin[k\pi\frac{x-a_1-d}{a_2}]}{[1-(\frac{x-a}{a_2})^2]^{1/3}}, \quad k = 1, 2, 3 \ldots \tag{44}$$

The transformed functions $\tilde{Q}$ and $\tilde{P}$ in each of the regions are given in terms of Bessel functions of the first kind of order 1/6 [16].

$$\tilde{P}_{k1}(m) = \frac{1}{2}\frac{a_1}{a}\Gamma(1/2)\Gamma(2/3)[\frac{J_{1/6}(\pi|m\frac{a_1}{a}-k|)}{(\pi/2|m\frac{a_1}{a}-k|)^{1/6}} - \frac{J_{1/6}(\pi(m\frac{a_1}{a}+k))}{(\pi/2(m\frac{a_1}{a}+k))^{1/6}}] \tag{45}$$

$$\tilde{P}_{k2}(m) = \frac{1}{2}\Gamma(1/2)\Gamma(2/3)[\frac{J_{1/6}(\pi|m-k|)}{(\pi/2|m-k|)^{1/6}} - \frac{J_{1/6}(\pi(m+k))}{(\pi/2(m+k))^{1/6}}] \tag{46}$$

$$\tilde{Q}_{k1}(m) = \frac{1}{2}\frac{a_2}{a}\Gamma(1/2)\Gamma(2/3)[\frac{J_{1/6}(\pi|m\frac{a_2}{a}-k|)}{(\pi/2|m\frac{a_1}{a}-k|)^{1/6}} - \frac{J_{1/6}(\pi(m\frac{a_2}{a}+k))}{(\pi/2(m\frac{a_2}{a}+k))^{1/6}}] \tag{47}$$

and

$$\tilde{Q}_{k2}(m) = (-1)^{k+m}\tilde{P}_{k2}(m) \tag{48}$$

The sums involved in the entries of the matrices in equations (38) contain terms in Bessel functions whose arguments are large (larger than 4). Asymptotic expressions of these functions can be fruitfully used to quicken the computations of these sums. It is also possible to use the 'static' sums in connection with established techniques in computing ζ-function to further reduce the CPU time [17]. This issue is not addressed in this paper, as only small matrices are needed, but becomes important as the number of discontinuities analyzed using the present technique becomes large.

V. RESULTS AND DISCUSSION

The CIET is applied to a variety of configurations in order to establish its efficiency and validity. In all figures, the solid line is obtained with 5 basis functions, the dotted line with 3 basis functions, the dashed line with 2 basis functions and the dotted-dahed line with one basis function.

The first structure we consider is an H-plane bifurcation as shown in Figure 1c. Only the fundamental mode TE_{10} is assumed incident from the left side. The equations describing the scattering phenomenon are presented in Appendix B.

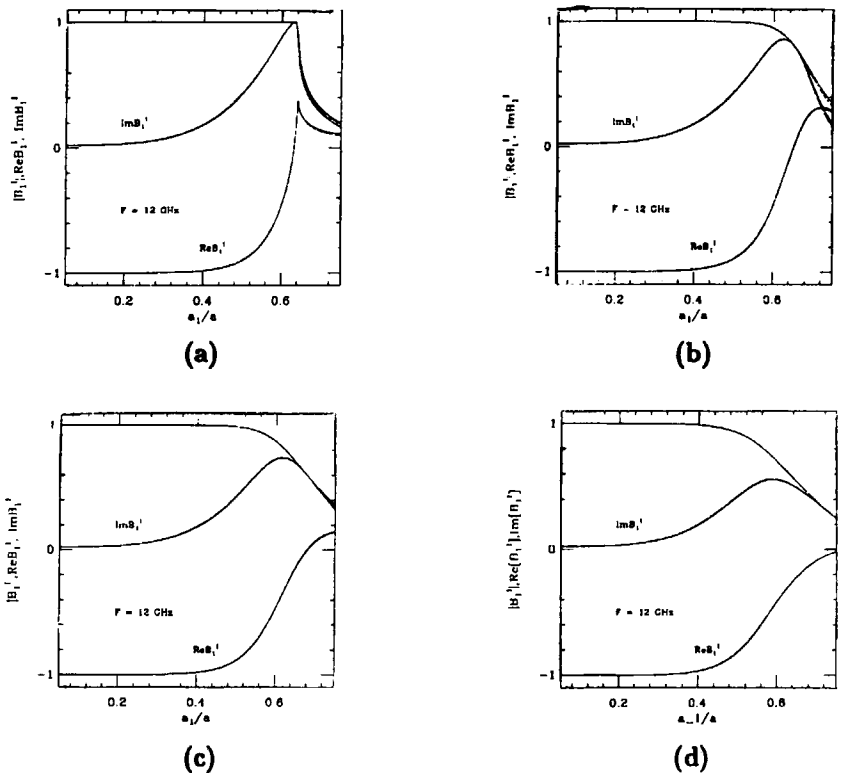

Figure 2. Magnitude, real part and imaginary part of B_1^I as a function of a_1/a for a bifurcation at 12 GHz and $a = 2b = 19.5$ mm, $a2 = 4.8$ mm for $M = 1, 2, 3$ and 5 basis functions. a) $L = \infty$, b) $L = 10$ mm, c) $L = 5$ mm and d) $L = 1$ mm.

Figure 2a shows the reflection coefficient B_1^I of an infinitely long ($L \rightarrow \infty$) bifurcations as a function of a_1/a while the width of the second bifurcation (a_2) is kept equal to 4.8 mm at 12 GHz (a=2b=19.5mm, $a_2 = 4.8$ mm). It can be clearly seen that the magnitude of the reflection coefficient is accurately predicted to be unity until one of the bifurcations is wide enough for the TE_{10} mode to propagate, i.e., when $a_1/a \geq 0.64058$. The convergence of the numerical solution is also evident as the difference between the results with M = 1 and M = 5 basis functions are minor over the entire range of a_1/a.

Figure 2b shows the same quantity for a bifurcation of length L=10 mm. As expected, the decrease of the magnitude of the reflection coefficient is now gradual and shows more structure after cutoff (a_1/a=0.64058) due to interference between the incident and reflected waves. The convergence of the numerical solution can also be clearly seen as the curves obtained with M = 2 and M = 5 are practically indistinguishable. Similar conclusions can be drawn from Figures 2c and 2d which represent the reflection coefficient for L=5 mm and L = 1 mm

respectively. It is worth mentioning that the strength of the interaction between adjacent discontinuities is accurately taken into account as can be seen from the convergence of the numerical solution when L is decreased. In the MMT, large individual scattering matrices are needed to accurately describe such interactions.

To further test the technique, we analyze two and three cascaded septums. Figures 3 show the reflected and transmitted power from two septums for typical dimensions and M = 1, 2, 3, 4 and 5 basis functions at each of the discontinuities. Figure 3a is a plot of the reflection coefficient as a function of the width of the gap a_1/a when the septums are 5 mm thick and separated by a distance of 1mm. The convergence of the solution is again evident. Figure 3b shows the same quantity when the two septums are 5 mm thick and separated by a distance of 5 mm.

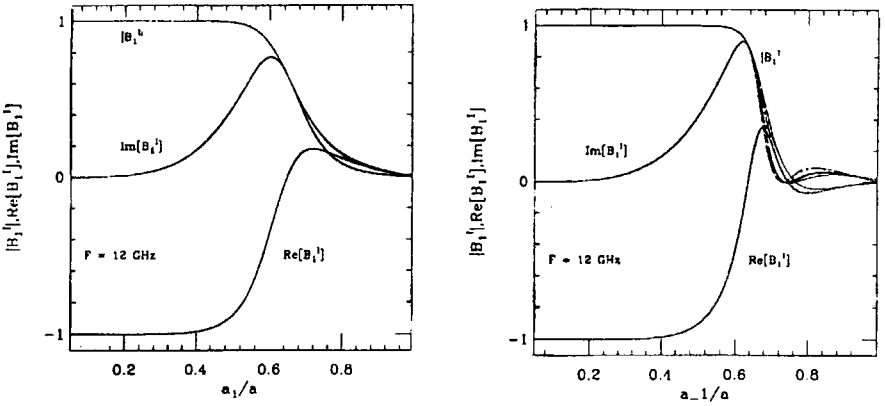

Figure 3: Magnitude, real part and imaginary part of B_1^I of two septums with $a = 2b = 19.5$ mm for $M = 1, 2, 3$, and 5 basis functions. a) as a function of a_1/a at 12 GHz with $d_1 = d_3 = 14$ mm and $d_2 = 5$ mm b) $d_1 = d_3 = 5$ mm and $d_2 = 5$ mm

We also examined the frequency response of the same structure over the frequency range of propagation of the fundamental mode TE_{10}. Figure 4 shows the reflection coefficient as a function of frequency when a_1 =11 mm and $a = 2b =$ 19.5 mm. The convergence of the numerical solution over the range of propagation of the fundamental mode, 7.68 GHz $\leq$ F $\leq$ 15.38 GHz, is documented as the results obtained with one and 5 basis functions practically coincide. It is also interesting to note that the local behavior of the real and imaginary parts, especially at points where either one is changing rapidly such as at the onset of the second mode at F = 15.38 GHz, reflect well the causality conditions [18]. These conditions, often referred to as Kramers-Kronig relations, relate the real and imaginary parts of any response function of a linear time invariant and causal physical system and can be used to test the plausibility of a given response function [19].

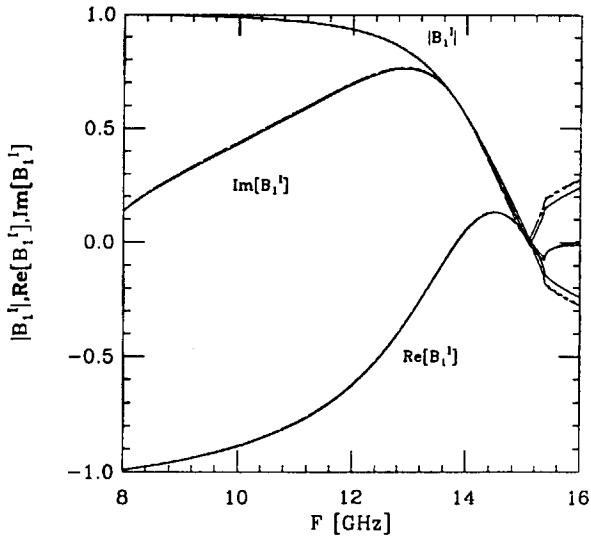

Figure 4: Magnitude, real part and imaginary part of B_1^I of two septums as a function of frequency for $M = 1, 2, 3$ and 5 basis functions with $a = 2b = 19.5$ mm, $a_1 = 11$ mm, $d_1 = d_3 = 1$ mm and $d_2 = 5$ mm.

A more stringent test is presented by the three septums of Figure 1b. The CIET allows the analysis of the entire structure in one step regardless of the dimensions and the location of the septums. Figures 5 show the reflection coefficient of the structure. Figure 5a is a plot of the magnitude, the real and the imaginary parts of B_1^I as a function of the width of the gap a_1/a at 12 GHz and with $a = 2b = 19.5$ mm. The septums are 5 mm thick and separated by a distance of 1 mm. As in the case of two septums, the convergence of the numerical solution is well documented. Two basis functions are sufficient to accurately determined the reflection (transmission) properties of the structure. The interference of incident and reflected waves result in a richer reflection characteristics especially when the gaps are large enough to allow the incident fundamental mode to propagate through the system. Figure 5b shows the same quantity when the septums are 5 mm thick and separated by a distance of 5 mm. Similar conclusions to those about Figure 5a hold for this case.

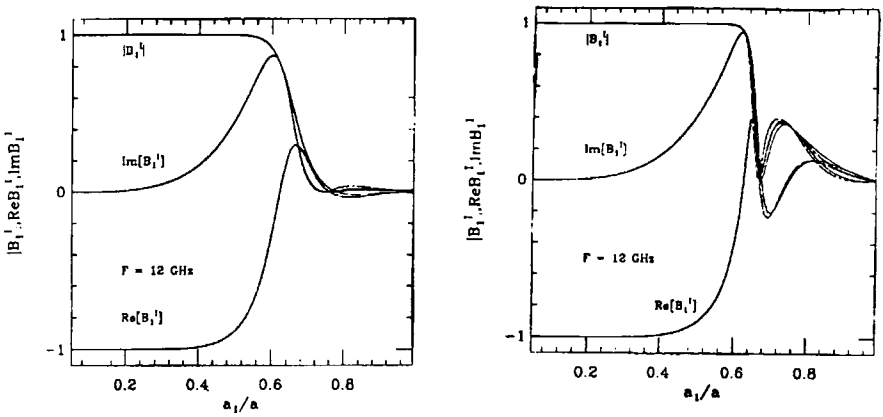

Figure 5: Magnitude, real part and imaginary part of B_1^I of three septums as a function of a_1/a with $a = 2b = 19.5$ mm for $M = 1, 2, 3$ and 5 basis functions at 12 GHz. a) $D - 1 = d_3 = d_5 = 1$ mm and $d_2 = d_4 = 5$ mm b) $d_1 = d_3 = d_5 = 5$ mm and $d_2 = d_4 = 5$ mm.

The frequency response of the system is shown in Figure 6. Over the entire range of propagation of the fundamental TE_{10} mode in the larger waveguide, one or at most two basis functions, are sufficient. Also, the causal properties of the real and imaginary parts of the system are properly reflected by these results in the vicinity of frequencies where either of the two quantities is rapidly varying such that its Hilbert transform is dominated by its local behavior.

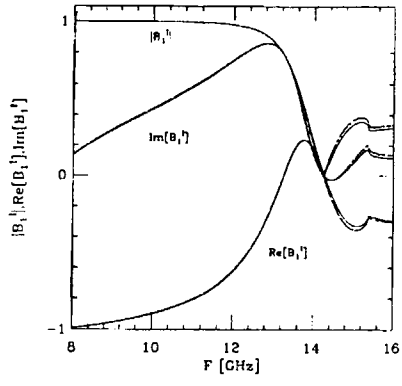

Figure 6: magnitude, real part and imaginary part of B_1^I of two septums as a function of frequency for $M = 1, 2, 3$ and 5 basis functions and $a = 2b = 19.5$ mm, $a_1 = 11$ mm, $d_1 = d_3 = d_5 = 1$ mm and $d_2 = d_4 = 5$ mm.

VI. CONCLUSIONS

The Coupled-Integral-Equations Technique (CIET) was applied to accurately determine the reflection properties of multiple discontinuities in rectangular waveguides. A set of coupled integral equations for the tangential electric field at the discontinuities are derived and then solved by the moment method. Basis functions which include the edge conditions and mirror images in the walls of the waveguide were used to accelerate the convergence of the numerical solution. The technique allows the determination of the overall response functions of multiple discontinuities without using the matrix representations for the individual discontinuities and regardless of the strength of their mutual interactions. A set of N discontinuities is accurately analyzed, and in one step, using a matrix of the order of $3N \times 3N$. Although only H-plane structures were considered, the technique is straightforwardly applied to E-plane and double-plane structures as well as cylindrical waveguides.

APPENDIX A

In this appendix we summarize the formulation for the analysis of three H-plane septums by the CIET. The structure and coordinate system are shown in Figure 1b. Let $X^{(i)}, i = 1, 2, ..6$ denote the unknown tangential electric fields at the interfaces, (see Figure 1b). Expanding the E_y in each of the seven regions in terms of the modes of the appropriate section of the waveguide and expressing the modal expansion coefficients in terms of the transformed functions $\tilde{X}^{(i)}$, and matching the tangential magnetic fields at each of the 6 interfaces, we get six coupled integral equations. The functions $X^{(i)}(x)$ are expanded in series of Basis functions, those used in the analysis of two septums as

$$X^{(i)}(x) = \sum_{k=1}^{M} c_k^{(i)} B_k(x) \tag{A.1}$$

Applying Galerkin's method to the integral equations, we get six sets of linear equations in the expansion coefficients

$$[A][c^{(1)}] + [B][c^{(2)}] = [U] \tag{A.2.a}$$

$$[C][c^{(1)}]] + [D][c^{(2)}] + [E][c^{(3)}] = 0 \tag{A.2.b}$$

$$[F][c^{(2)}] + [G][c^{(3)}] + [H][c^{(4)}] = 0 \tag{A.2.c}$$

$$[I][c^{(3)}] + [J][c^{(4)}] + [K][c^{(5)}] = 0 \tag{A.2.d}$$

$$[L][c^{(4)}] + [M][c^{(5)}] + [N][c^{(6)}] = 0 \tag{A.2.e}$$

$$[O][c^{(5)}] + [P][c^{(6)}] = 0 \tag{A.2.f}$$

The entries of the matrices are given by the following expressions

$$[A]_{kl} = \sum_{m=1}^{\infty} [Y_m^I \tilde{B}_{k1}(m)\tilde{B} - l1(m) - j\frac{a_1}{a} Y_m^{II} \cot(k_m^{II} d_1) \tilde{B}_{k2}(m)\tilde{B}_{l2}(m)] \tag{A.3.1}$$

$$[B]_{kl} = j\frac{a_1}{a}\sum_{m=1}^{\infty} Y_m^{II}\frac{\tilde{B}_{k2}(m)\tilde{B}_{l2}(m)}{\sin[k_m^{II}d_1]} \tag{A.3.2}$$

$$[U]_k = 2Y_1^I]\tilde{B}_{k1}(1) \tag{A.3.3}$$

$$[C]_{kl} = \frac{a_1}{a}\sum_{m=1}^{\infty} Y_m^{II}\frac{\tilde{B}_{k2}(m)\tilde{B}_{l2}(m)}{\sin[k_m^{II}d_1]} \tag{A.3.4}$$

$$[D]_{kl} = -\sum_{m=1}^{\infty}[Y_m^I\tilde{B}_{k1}(m)\tilde{B}_{l1}(m)\cot(k_m^I d_2) + \frac{a_1}{a}Y_m^{II}\tilde{B}_{k2}(m)\tilde{B}_{l2}(m)\cot(k_m^{II}d_1)] \tag{A.3.5}$$

$$[E]_{kl} = \sum_{m=1}^{\infty} Y_m^I\frac{\tilde{B}_{k1}(m)\tilde{B}_{l1}(m)}{\sin[k_m^I d_2]} \tag{A.3.6}$$

$$[F] = [E] \tag{A.3.7}$$

$$[G]_{kl} = -\sum_{m=1}^{\infty}[Y_m^I\tilde{B}_{k1}(m)\tilde{B}_{l1}(m)\cot(k_m^I d_2) + \frac{a_1}{a}\tilde{B}_{k2}(m)\tilde{B}_{l2}(m)\cot(k_m^{II}d_3)] \tag{A.3.8}$$

$$[H]_{kl} = \frac{a_1}{a}\sum_{m=1}^{\infty} Y_m^{II}\frac{\tilde{B}_{k2}(m)\tilde{B}_{l2}(m)}{\sin[k_m^{II}d_3]} \tag{A.3.9}$$

$$[I] = [H] \tag{A.3.10}$$

$$[J]_{kl} = -\sum_{m=1}^{\infty}[Y_m^I\tilde{B}_{k1}(m)\tilde{B}_{l1}(m)\cot(k_m^I d_4) + \frac{a_1}{a}Y_m^{II}\tilde{B}_{k2}(m)\tilde{B}_{l2}(m)\cot(k_m^{II}d_3)] \tag{A.3.11}$$

$$[K]_{kl} = \sum_{m=1}^{\infty} Y_m^I\frac{\tilde{B}_{k1}(m)\tilde{B}_{l1}(m)}{\sin[k_m^I d_4]} \tag{A.3.12}$$

$$[L] = [K] \tag{A.3.13}$$

$$[M]_{kl} = \sum_{m=1}^{\infty}[Y_m^I\tilde{B}_{k1}(m)\tilde{B}_{l1}(m)\cot(k_m^I d_4) + \frac{a_1}{a}Y_m^{II}\tilde{B}_{k2}(m)\tilde{B}_{l2}(m)\cot(k_m^{II}d_3)] \tag{A.3.14}$$

$$[N]_{kl} = \frac{a_1}{a}\sum_{m=1}^{\infty} Y_m^{II}\frac{\tilde{B}_{k2}(m)\tilde{B}_{l2}(m)}{\sin[k_m^{II}d_5]} \tag{A.3.15}$$

$$[O]_{kl} = j[N]_{kl} \tag{A.3.16}$$

and

$$[P]_{kl} = \sum_{m=1}^{\infty}[Y_m^I\tilde{B}_{k1}(m)\tilde{B}_{l1}(m) - j\frac{a_1}{a}Y_m^{II}\tilde{B}_{k2}(m)\tilde{B}_{l2}(m)\cot(k_m^{II}d_5)] \tag{A.3.17}$$

The basis functions and their transformed are given in equations (20) and (21) respectively.

APPENDIX B

This appendix groups the main results for an infinitely long bifurcation ($L \rightarrow \infty$ in Figure 1c).

The tangential electric field at the two interfaces is denoted by $Z^{(1)}(x)$ and $Z^{(2)}(x)$ respectively. By following the same steps as those that led to the integral equations for a bifurcation of finite length, two coupled integral equations are derived for $Z^{(1)}(x)$ and and $Z^{(2)}(x)$, namely

$$\sum_{m=1}^{\infty} Y_m^I[\tilde{Z}_1^{(1)}(m) + \tilde{Z}_1^{(2)}(m)] \sin[m\pi\frac{x}{a}] + \sum_{m=1}^{\infty} Y_m^{II} \tilde{Z}_2^{(1)}(m) \sin[m\pi\frac{x}{a_1}] = 2Y_1^I \sin[\pi\frac{x}{a}], \quad 0 \leq x \leq a_1 \tag{B.1.1}$$

and

$$\sum_{m=1}^{\infty} Y_m^I[\tilde{Z}_1^{(1)}(m) + \tilde{Z}_1^{(2)}(m)] \sin[m\pi\frac{x}{a}] + \sum_{m=1}^{\infty} Y_m^{III} \tilde{Z}_3^{(1)}(m) \sin[m\pi\frac{x-a_1-d}{a_2}] = 2Y_1^I \sin[\pi\frac{x}{a}], \quad a_1 + d \leq x \leq a. \tag{B.1.2}$$

Expanding the functions in series of basis functions $P_k(x)$ and $Q_k(x)$ as in equations (30) and (31) and applying Galerkin's method, we get two linear sets of equations in the expansions coefficients $a^{(1)}$ and $a^{(2)}$

$$[A][a^{(1)}] + [B][a^{(1)}] = [U] \tag{B.2.1}$$

and

$$[C][a^{(1)}] + [D][a^{(1)}] = [V] \tag{B.2.2}$$

where the matrices are given by

$$[A]_{kl} = \sum_{m=1}^{\infty} [Y_m^I \tilde{P}_{k1}(m) \tilde{P}_{l1}(m) + \frac{a_1}{a} Y_m^{II} \tilde{P}_{k2}(m) \tilde{P}_{l2}(m)] \tag{B.3.1}$$

$$[B]_{kl} = \sum_{m=1}^{\infty} Y_m^I \tilde{P}_{k1}(m) \tilde{Q}_{l1}(m) \tag{B.3.2}$$

$$[U]_k = 2Y_1^I \tilde{P}_{k1}(1) \tag{B.3.3}$$

$$[C]_{kl} = [B]_{lk} \tag{B.3.4}$$

$$[D]_{kl} = \sum_{m=1}^{\infty} [Y_m^I \tilde{Q}_{k1}(m) \tilde{Q}_{l1}(m) + \frac{a_1}{a} Y_m^{II} \tilde{Q}_{k2}(m) \tilde{Q}_{l2}(m)] \tag{B.3.5}$$

and

$$[V]_k = 2Y_1^I \tilde{Q}_{k1}(1) \tag{B.3.6}$$

REFERENCES

1. Marcuvitz, N., *Waveguide Handbook*, McGraw-Hill, New York, 1951.
2. Schwinger, J., and D. S. Saxon, *Discontinuities in Waveguides*, Gordon & Breach, New York, 1968.
3. Wexler, A., "Solution of waveguide discontinuities by modal analysis," *IEEE Trans. Microwave Theory Tech.*, Vol. MTT-15, 508-517, Feb. 1967.
4. Uher, J., J. Bornemann, and U. Rosenberg, *Waveguide Components for Antenna Feed Systems: Theory and CAD*, Artech House, Boston 1993.
5. Auda, H., and R. F. Harrington, "A moment solution for waveguide junction problems," *IEEE Trans. Microwave Theory Tech.*, Vol. MTT-31, 515–519, July 1972.
6. Leong, M. S., P. S. Kooi, and Chandra, "A new class of basis functions for the solution of the E-plane waveguide discontinuity problem," *IEEE Trans. Microwave Theory Tech.*, Vol. MTT-35, 705–709, July 1987.
7. Lyapin, V. P., V. S. Mikhalevsky, and G. P. Sinyavsky, "Taking into account the edge condition in the problem of diffraction of waves on step discontinuity in plate waveguide," *IEEE Trans. Microwave Theory Tech.*, Vol. MTT–30, 1107–1109, 1982.
8. Itoh, T., ed., *Numerical Techniques for Microwave and Millimeter-Wave Passive Structures*, John Wiley & Sons, New York 1989.
9. Sorrentino, R., M. Mongiardo, F. Alessandri, and G. Schiovon, "An investigation of the numerical properties of the Mode-Matching Technique," *Int. Jour. Numerical Modelling*, Vol. 4, 19–43, March 1991.
10. Mongiardo, M., and T. Rozzi, "Singular integral equation analysis of flange-mounted rectangular waveguide radiators," *IEEE Trans. Antennas Propagat.*, Vol. 41, 556–565, May 1993.
11. Yang, R., and A. S. Omar, "Rigorous analysis of iris coupling problems in waveguide," *IEEE Trans. Microwave Theory Tech.*, Vol. MTT-41, 349–352, Feb. 1993.
12. Harrington, R. F., *Time Harmonic Electromagnetic Fields*, McGrawHill, New York 1969.
13. Alessandri, F., M. Mongiardo, and R. Sorrentino, "Computer-aided design of beam forming networks for modern satellite antennas," *IEEE Trans. Microwave Theory Tech.*, Vol. MTT-40, 1117–1127, June 1992.
14. Harrington, R. F., *Field Computation by Moment Methods*, Krieger, Malabar, Florida 1987.
15. Collin, R. E., *Field Theory of Guided Waves*, IEEE Press, New York, 1991.
16. Gradshteyn, I. S., and I. M. Ryznik, *Tables of Integrals, Series, and Products*, Fifth Edition, Academic Press, New York, 1994.
17. Bender, C. M., and S. A. Orszag, *Advanced Mathematical Methods for Scientists and Engineers*, McGrawHill, New York, 1978.
18. Ziman, J. M., *Principles of the Theory of Solids*, Cambridge Univ. Press, London, 1964.
19. Amari, S., M. Gimersky, and Bornemann, "Imaginary part of antenna's admittance from its real part using Bode's integrals," *IEEE Trans. Antennas and Propag.* Vol. 43, 220–223, Feb. 1995.

Smain Amari received his DES in Physics and Electronics from Constantine University (Algeria) in 1985, the MS degree in Electrical Engineering in 1989 and the Ph.D. degree in Physics in 1994 both from Washington University in St. Louis. he is interested in numerical methods of electromagnetics, numerical analysis, applied mathematics, applied physics, and application of quantum field theory in quantum many-particle systems.

Jens Bornemann received the Dipl.-Ing. and Dr.-Ing. degrees in electrical engineering from the University of Bremen, germany in 1980 and 1984, respectively. He is currently a Professor in the Department of ECE, University of Victoria, B.C., Canada. His research

activities focus on microwave components design, and electromagnetic field theory in circuits and antennas. Dr. Bornemann is a Senior Member of IEEE and serves on the editorial boards of *IEEE Trans. MTT* and *Int. J. of Numerical Modelling*. He has (co)authored more than 100 technical papers and a book on *Waveguide Components for Antenna Feed Systems–Theory and CAD*, Artech House, 1993.

Rüdiger Vahldeick (M'85–SM'86) received the Dipl.-Ing. and Dr.-Ing. degrees in electrical engineering from the University of Bremen, West Germany, in 1980 and 1983, respectively. From 1984 to 1986 he was a Research Associate at the University of Ottawa, Canada. In 1986 he joined the University of Victoria, British Columbia, Canada, where he is now a Full Professor in the Department of Electrical and Computer Engineering. During Fall and Spring 1992-93 he was a visiting scientist at the "Ferdinand-Braun-Institute für Hochfrequenztechnik" in Berlin, germany. His research interests include numerical methods to electromagnetic fields for computer-aided design of microwave, millimeter wave, and opto-electronic integrated circuits. He is also interested in the design and simulation of devices and subsystems for broadband fiber-optic communication systems. He is on the editorial board of the *IEEE Transaction on Microwave Theory and Techniques* and has published more than 100 technical papers mainly in the fields on microwave CAD.